Dalton Transactions

Accepted Manuscript

This article can be cited before page numbers have been issued, to do this please use: I. -. GUPTA, N. Manav, P. E. Kesavan, M. Ishida , S. Mori, Y. Yasutake, S. Fukatsu and H. Furuta, *Dalton Trans.*, 2019, DOI: 10.1039/C8DT04540B.

ROYAL SOCIETY OF CHEMISTRY

rsc.li/dalton

ROYAL SOCIETY OF CHEMISTRY View Article Online
DOI: 10.1039/C8DT04540B

Journal Name

ARTICLE

Phosphorescent Rhenium-Dipyrrinates: Efficient Photosensitizers for Singlet Oxygen Generation

fReceived 00th November 20xx,
Accepted 00th November 20xx

DOI: 10.1039/x0xx00000x

www.rsc.org/

Neha Manav,[a] Praseetha E. Kesavan,[a] Masatoshi Ishida,[b] Shigeki Mori,[c] Yuhsuke Yasutake,[d] Susumu Fukatsu,[d] Hiroyuki Furuta,[b] and Iti Gupta*[a]

A series of rhenium(I) dipyrrinato complexes (**Re1–Re8**) have been prepared and characterized; their crystal structures, phosphorescence and singlet oxygen generation studies are reported. The aromatic substituents, such as thienyl, *p*-bromophenyl, *p*-fluorophenyl, *m*-fluorophenyl, pentaflurophenyl, *N*-butylcarbazole, *N*-phenylcarbazole, and *N*-butylphenothiazine, are linked to the C5 position of Re-dipyrrinates. Varying the electronic nature of substituents from electron donating (e.g., carbazole) to electron withdrawing (e.g., pentaflurophenyl) allowed the change in the structural, electrochemical, and spectroscopic properties in these complexes. In particular, the Rhenium dipyrrinates showed phosphorescence in the near IR region with sufficiently longer triplet state lifetimes (τ_T = 9–29 μs). Also, large Stokes shifts ($\Delta\nu$ = 5682–6957 cm^{-1}) were witnessed for all the rhenium dipyrrinates. Triplet emission reflected in the efficient singlet oxygen generation yields (Φ_Δ ~ 0.75–0.98) along with the distinct photo-stability. Density functional theory (DFT) calculations revealed that the electron density is spread over dipyrrin unit in most of the complexes. Rhenium dipyrrinate having a phenothiazine substituent exhibited the smallest HOMO-LUMO band gap (2.820 eV) among all the Re-complexes.

Introduction

In past three decades, the chemistry of dipyrromethanes has gained popularity[1, 2] primarily because they have been used as key precursors for preparation of various porphyrins, corroles and norcorroles.[3-7] The oxidized form of dipyrromethane is known as dipyrromethene or dipyrrin that has emerged as a resourceful ligand in rich coordination chemistry;[8, 9] the planar dipyrrin unit consists of two nitrogen atoms as donor sites, which provide a versatile pattern for complexation to metal ions. Dipyrrins have been used as a bidentate nitrogen donating ligand to form stable metal complexes, i.e., metal dipyrrinato complexes.[10] To date, dipyrrins have been extensively used for the preparation of a wide range of boron difluoride dipyrromethene dyes (namely BODIPYs).[11] The highly emissive BODIPYs and their derivatives have found applications as biological labelling's, photosensitizers in PDT (photodynamic therapy)[12, 13] energy transfer systems, light harvesting devices and chemosensors.[14, 15] Extended conjugation across the two pyrrole rings in the dipyrrins makes them rich in photophysical and electrochemical properties and structural modifications were conducted to alter the spectrochemical properties of the ligand for different applications.

Not only for main group elements, variety of dipyrrinato complexes have been reported with 3rd-to-5th row transition metals.[16, 17] Nishihara and co-workers have used this feature and reported luminescent In(III) and Zn(II) containing heteroleptic complexes with high quantum yields.[18-20] The heavy transition metal dipyrrin complexes have potentials for the phosphorescent emitters in organic light emitting diodes (OLED) applications by taking advantage of their strong spin orbit couplings. In analogy to the well-known iridium(III)-based emitters, rhenium (I) complexes are also gathering attentions for OLED applications because of high photo-luminescence efficiency and short luminescence lifetime.[21] Recently, Roy and co-workers reported highly emissive tricarbonyl Re(I) phenanthroline complexes[22] with blue coloured solid state emission and their application in electroluminescent devices. Furthermore, a variety of Re(I) complexes have been developed for applications as luminescent bio-imaging probes[23, 24] and triplet sensitizers in photocatalysis,[25, 26] photovoltaics,[27] and triplet-triplet annihilation (TTA) upconversion. [28]

In an effort to seek the efficient light-harvesting capability, rhenium(I) dipyrrinato complexes prepared by Telfer and co-workers,[29, 30] which exhibited intense luminescence in the

[a] Indian Institute of Technology Gandhinagar, Palaj Campus, Gandhinagar, Gujarat-382355, India.
[b] Department of Chemistry and Biochemistry, Graduate School of Engineering and Center for Molecular Systems, Kyushu University, Fukuoka 819-0395, Japan
[c] Advanced Research Support Center, Ehime University, Matsuyama 790-8577, Japan,
[d] Graduate School of Arts and Sciences, The University of Tokyo, Tokyo 153-8902, Japan

† Footnotes relating to the title and/or authors should appear here.
Electronic Supplementary Information (ESI) available: [details of any supplementary information available should be included here]. See DOI: 10.1039/x0xx00000x

visible range and this property has been utilized in the area of solar energy conversion and biological labelling, and radio-imaging applications.[31, 32] Such heavy metal dipyrrin complexes can be used as photosensitizers for singlet oxygen generation ($^1\Delta_g$); which in turn can be used for water disinfection and photodynamic therapy (PDT).[33-35] In fact, ideal sensitizers require efficient $^1O_2$ generation quantum yields, good photostability under strong laser irradiation and high absorption coefficients in red region. However, there is a need to develop better singlet oxygen sensitizers for practical applications. In this regard, elucidation of the structure-property relationship of the Re(I) dipyrrinato complexes is of importance for the rational design of dual-modal molecules with high phosphorescence and singlet oxygen generation yields.

In this work, novel rhenium(I) dipyrrinato complexes possessing various electron-donor and withdrawing groups at the C5 position of the dipyrrin core such as 2-thienyl, *p*-bromophenyl, *p*-fluorophenyl, *m*-fluorophenyl, pentaflurophenyl, *N*-butylcarbazole, *N*-phenylcarbazole and *N*-butylphenothiazene are presented. The substitution effect on the photophysical and electrochemical properties of rhenium dipyrrinates has been discussed systematically. The phosphorescent emission lifetime, quantum yields and singlet oxygen generation ability of the complexes were analysed. Density functional theory (DFT-D3) calculations were conducted to understand the electronic structures in details.

Results and Discussion

Synthesis and characterization

As shown in the Scheme 1, the corresponding rhenium complexes (**Re1-Re8**) were synthesized in a stepwise manner. Firstly, the key precursor dipyrromethanes (**1-8**) having different electron-donating and withdrawing moieties were synthesized as per the literature reports.[36] The dipyrromethanes were then oxidized with *p*-chloranil in dry dichloromethane (DCM).[37] The resulting crude dipyrrins **1-8** were then purified by neutral alumina column chromatography. The pure dipyrrins were further treated with $Re(CO)_5Cl$ in toluene for 1 h, followed by the addition of triphenylphosphine in the presence of triethylamine (Scheme 1). The progress of the reaction was monitored by thin layer chromatography (TLC) and reaction was stopped when the dipyrrin was consumed. The reaction mixture was then subjected to neutral alumina column chromatography to obtain pure rhenium dipyrrinates, **Re1–Re8** as orange solid in 45-88% yields. All compounds were characterized by mass, IR, ^{1}H and ^{13}C NMR spectroscopies (*cf*. supplementary information). In the IR spectra of metal complexes **Re1**–**Re8**, energies of the vibrations observed were corresponded to the structure of the dipyrrins dependent on the functional groups.

The three characteristic C-O stretching vibrations (asymmetric and symmetric) for carbonyl groups were observed around 2020, 1926, 1896 cm^{-1} for Re1. This is the typical pattern observed for three CO units in *fac* isomer arrangements for all the rhenium dipyrrinates.[38]

Importantly, the wavenumbers of CO stretches are very sensitive to the electronic structures of the rhenium complexes, and the constancy of the wavenumbers suggests equal perturbation of the metal centre by various substituents on the dipyrrin core. Similar to the reported Re(I) dipyrrin complexes[29], the complexes, **Re1–Re8** contains low spin d^6 rhenium metal and all the compounds are diamagnetic. The ^{1}H and ^{13}C NMR spectra of the compounds **Re1–Re7** were recorded in $CDCl_3$, whereas for **Re8**, DMSO-d_6 was used due to the solubility issue (*cf*. supplementary information).

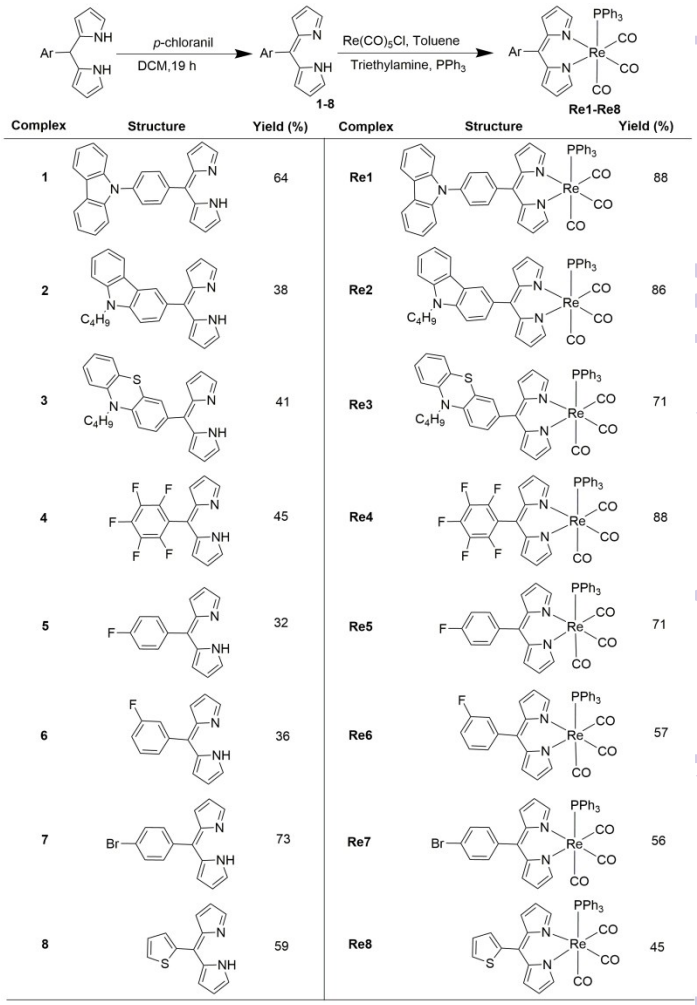

Scheme 1. Synthetic route for rhenium dipyrrinates (**Re1-Re8**).

^{31}P NMR spectra of compounds **Re1-Re8** were recorded in $CDCl_3$ (*cf*. supplementary information). Typically, the free PPh_3 group in phosphorous NMR appear as a singlet around -6 ppm; whereas in case of **Re1-Re8** ^{31}P signal showed up between 10.55 to 15.84 ppm (*cf*. supplementary information). The downfield shift in phosphorous NMR signal w.r.t free PPh_3 ligand can be explained on the basis of lower electron density on P atom due to metal complexation in **Re1-Re8.** However, the electron withdrawing or electron donating nature of the substitutents at the C5-position of dipyrrin unit had little effect on the chemical shift values of ^{31}P signal in these compounds.

View Article Online
DOI: 10.1039/C8DT04540B

Single Crystal X-ray Diffraction Analysis

The structures of the six rhenium dipyrrinates **Re1** and **Re3–Re7** were established by X-ray crystallographic analysis (Figure 1 and Table S2). ORTEP views of the solved crystal structures are presented in Figure 1 and the selected bond lengths and torsion angles are given in Table 1. The colour of the crystals of **Re1** and **Re4** were orange and red respectively with $P2_1/n$ (#14) space group. **Re3** and **Re7** gave orange plate crystals with $P2_1/c$ (#14) space group. **Re5** and **Re6** produced orange plate crystals with *Ia* (#9) space group. The compounds, **Re1** and **Re3-Re7** displayed monoclinic crystal system. These rhenium dipyrrinates have distorted octahedral geometry about rhenium(I) centre and possess C_s symmetry. The dipyrrin core is substantially lying in the same plane as that of rhenium centre and two carbonyl ligands. The PPh_3 and third carbonyl ligand are spread out in opposite directions, in *trans* position and both are perpendicular to the dipyrrin plane. The Re-N1 and Re-N2 bond distances were between 2.15(5) to 2.18(6) Å; the N1-Re-N2 bond angles were in the range of 84.25(11)° to 85.08(2)° in these complexes. The observed Re-N (dipyrrin) distances were slightly shorter than the reported rhenium dipyrrinato complexes. The Re-P (phosphine) lengths were in the range of 2.479(5) to 2.528(2) Å; these values were marginally higher than the reported Re-P distances of mixed ligand Re(I) dicarbonyl complexes.[39] The Re-C(O) distances between Re and carbonyl groups were in the range of 1.916(2) to 1.968(18) Å, these values are comparable with the previous report.[29]

Generally a donor group *trans* to CO would be expected to cause weakening of CO bond, which can be reflected in the increase of C-O bond lengths. However, the C-O bond lengths appeared to be similar ranging from 1.139(8) to 1.152(6) Å for the carbonyls opposite to dipyrrinato ligand in the complexes. Also, the C-O bond lengths of carbonyls *trans* to phosphine group were between 1.119(8) to 1.152(9) Å; thus regardless of the *trans* ligand bonds of similar nature are of comparable length across the series of rhenium dipyrrinates (Table 1). For **Re1, Re3** and **Re4** the torsion angles [C6-C5-C10-C15, C4-C5-C10-C11] between the dipyrrin plane and the bulky aromatic group at C5 position were between 63.7(7)° to 66.3(4)°. For **Re5** and **Re6** the dihedral angles [C6-C5-C10-C15, C4-C5-C10-C11] were in the range of 68.8(16)° to 73.4(8)°; these torsion angle values were slightly higher than the **Re1**. The higher values of dihedral angle [C6-C5-C10-C15, C4-C5-C10-C11] 80.9(5)° and 83.3(5)° were observed for **Re7** having 4-bromophenyl group on the dipyrrin core. The higher degree of torsion angles between C5 aromatic moieties and the dipyrrin core indicated less effective electronic interactions between the two units in compounds **Re5**, **Re6** and **Re7**.

Photophysical Properties

The UV-vis absorption studies of the complexes were carried out in toluene and the data are presented in Table 2. As shown in Figure 2, all complexes exhibited an intense absorption band centred around 490–500 nm. This strong absorption band arises due to S_0 to S_1 transition (primarily π-π^*) of dipyrrin ligand.[40-42]

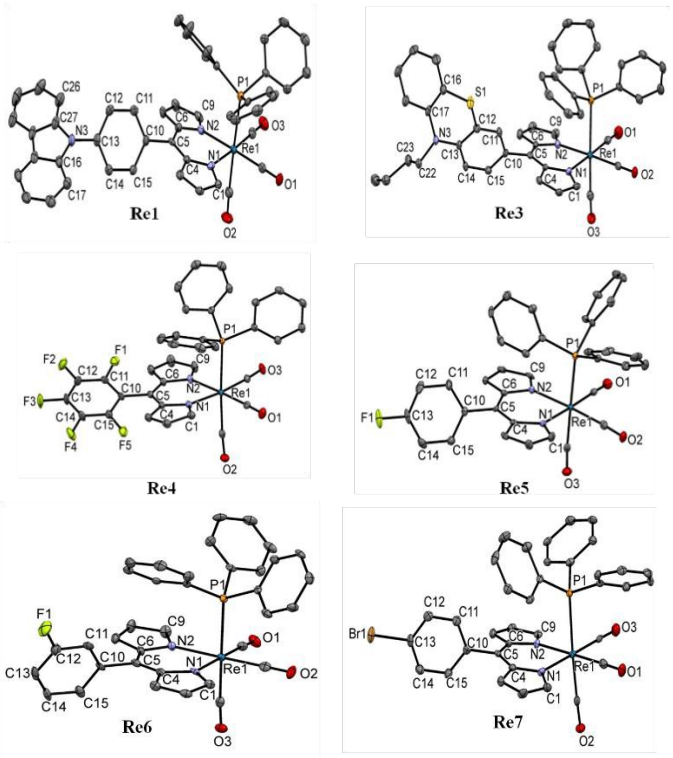

Figure 1. ORTEP representations (50% probability level) of the single crystal X-ray structures of **Re1** and **Re3–Re7**. Hydrogen atoms are omitted for clarity.

The corresponding extinction coefficients (ε) of the major absorption bands are in the range of 22,000 to 39,000 $M^{-1}cm^{-1}$. Small shoulders are also present in the absorption spectra around 400–420 nm in all the rhenium dipyrrinates, which are attributed to the S_0 to S_2 transitions centred on dipyrrin unit. This absorption feature is akin to the reported iridium-dipyrrinato complexes;[43] which indicates that the transition energy of the major absorption band is relatively insensitive to the identity of metal ion.[44] The high intensity low energy absorption bands of **Re1-Re8** were significantly red shifted (~125 nm) w.r.t. the phenanthroline Re(I) tricarbonyl complexes bearing one water soluble phosphine group.[45] Whereas, the absorption maxima of low energy band of **Re1-Re8** displayed about 40-60 nm red shifts w.r.t. Re(I) tricarbonyl complexes having single 1,10-phenanthroline or 2,2'-bipyridyl groups.[38, 46] The considerable red shifts could be attributed to the presence of dipyrrin ligand in **Re1-Re8,** which is responsible for intra-ligand π-π^* transitions. The absorption maxima of major absorption band in **Re1-Re8** were ~60 nm red shifted in comparison to the triphenylamine substituted dipyrrinato Zn(II), Ni(II) and Pd(II) complexes; which may be due to the complexation of heavy metal Re(I) with the dipyrrin unit.[9]

View Article Online DOI: 10.1039/C8DT04549B

Table 1. Selected bond distances, bond angles and torsion angles of the rhenium dipyrrinates.

Complex	Dihedral Angles (°)	Bond Angles (°)	Bond Distances (Å)	
Re1	C4–C5–C10–C15 63.99(7) C6–C5–C10–C11 63.69(7)	N1–Re–N2 84.66(18)	Re–P1 2.523(15) Re–N1 2.150(5) Re–N2 2.153(4)	Re–C46 1.921(6) Re–C47 1.959(6) Re–C48 1.926(6)
Re3	C4–C5–C10–C11 66.28(4) C6–C5–C10–C15 64.00(4)	N1–Re–N2 84.27(11)	Re–P1 2.528(2) Re–N1 2.179(6) Re–N2 2.169(6)	Re–C44 1.926(7) Re–C45 1.932(8) Re–C46 1.935(8)
Re4	C4–C5–C10–C11 65.46(2) C6–C5–C10–C15 64.17(2)	N1–Re–N2 84.48(6)	Re–P1 2.479(5) Re–N1 2.168(18) Re–N2 2.172(15)	Re–C34 1.925(18) Re–C35 1.968(18) Re–C36 1.916(2)
Re5	C4–C5–C10–C15 73.47(8) C6–C5–C10–C11 71.84(8)	N1–Re–N2 84.72(2)	Re–P1 2.524(19) Re–N1 2.168(5) Re–N2 2.172(5)	Re–C34 1.934(7) Re–C35 1.934(7) Re–C36 1.947(7)
Re6	C4–C5–C10–C11 68.77(16) C6–C5–C10–C15 73.05(16)	N1–Re–N2 85.08(2)	Re–P1 2.528(2) Re–N1 2.180(6) Re–N2 2.169(6)	Re–C34 1.930(7) Re–C35 1.938(8) Re–C36 1.934(8)
Re7	C4–C5–C10–C11 83.35(5) C6–C5–C10–C15 80.93(5)	N1–Re–N2 84.25(14)	Re–P1 2.527(12) Re–N1 2.160(4) Re–N2 2.160(4)	Re–C34 1.932(5) Re–C35 1.941(5) Re–C36 1.923(5)

Furthermore, the comparison of absorbance spectra of complexes revealed that, various *meso*-substituents at C5 position of the dipyrrin ligand did not cause significant shifts in their absorption. Whether the substituents at C5 position of dipyrrin unit are electron rich bulky aromatic groups such as carbazole or phenothiazine derivatives (in **Re1-Re3**) or electron withdrawing halobenzene groups (in **Re5-Re7**); they have negligible influence on the absorption maxima. This trend is analogous to the previously reported metal-dipyrrinato complexes.[44, 45] However, the **Re4** and **Re8** exhibited 11-12 nm red shifts in the absorption band as compared to the reported *meso*-phenyl rhenium(I) dipyrrinato complex (489 nm).[29]

Metal dipyrrinato complexes containing heavy metals like Re(I), Ir(III), Pt(II) and Ru(II) are known to be phosphorescent in nature with potential applications in materials and biology.[16, 17, 43, 47, 48] Luminescent properties of the complexes, **Re1–Re8** were observed at room temperature in deaerated toluene (Figure 2). All complexes showed vibrationally structured emission spectra with an intense peak around 680-736 nm and a moderate band between 743-814 nm. The negligible fluorescence could be ascribed to the rapid singlet-triplet intersystem crossing in these rhenium dipyrrinates. The relative quantum yields calculated for **Re1-Re8** were quite low (in witnessed for all the rhenium dipyrrinates and the values were in the range of 5682-6957 cm^{-1}. The bulky electron rich aromatic groups like carbazole and phosphine derivatives on the *meso*-position of dipyrrin unit (in **Re1-Re3**) displayed high energy phosphorescence maxima between 681-692 nm with relatively smaller Stokes shift. On the other hand, electron withdrawing halobenzene groups on the *meso*-position of dipyrrin unit exhibited lower energy phosphorescence maxima around 698-736 nm with fairly larger Stokes shift. The lowest energy phosphorescence band was observed at 736 nm for **Re4** having an electron withdrawing pentafluorophenyl moiety on the C5 position of dipyrrin unit.

Table 2. Absorption data (in Toluene) and phosphorescence data (in toluene) of rhenium dipyrrinates.

Complex	λ_{abs} (nm), log ε	λ_{em} (nm)	Stokes shift (cm^{-1})	Φ_{PL} [a] (%)	τ_{PL} [b] (μs)	k_r (10^3 s^{-1})	k_{nr} (10^3 s^{-1})
Re1	492, 4.51	692, 755	5874	0.001	8.0	2.87	122.12
Re2	491, 4.59	681, 743	5682	0.002	29.0	1.54	19.03
Re3	493, 4.34	688, 749	5749	0.006	9.0	3.60	107.51
Re4	500, 4.52	736, 814	6413	0.001	4.2	2.19	235.90
Re5	492, 4.56	690, 748	5742	0.002	17.5	1.59	55.55
Re6	493, 4.55	698, 755	6957	0.002	11.7	1.36	84.11
Re7	492, 4.51	695, 756	5847	0.002	14.0	1.53	69.90
Re8	501, 4.43	719, 789	6052	0.001	3.8	6.81	256.34

[a] λ_{ex} = 485 nm. Triphenylamine substituted corresponding rhenium dipyrrinate was used as standard [Φ_{PL} = 0.5% in DCM]. [b] λ_{ex} = 532 nm.

The phosphorescence decays of rhenium dipyrrinates were determined by TCSPC method and analyzed by monoexponential curve fittings. The microsecond time scale of the lifetimes (3.6 μs - 29 μs) supports that the emissions are originated from the triplet states (Table 2). **Re2** showed the relatively longer T_1 lifetime followed by **Re5** i.e., 29 μs and 17.5 μs respectively. All complexes showed higher values of non-radiative decay constant (k_{nr}) than the radiative one (Table 2). Higher values of Stokes shifts, long triplet

state lifetime at room temperature and the quenched emission quantum yield confirms the emission from excited triplet state of rhenium complexes.[29]

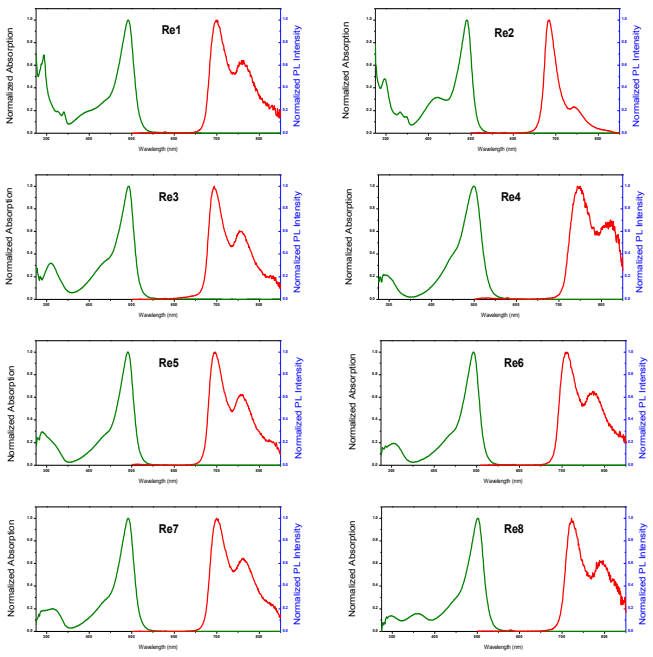

Figure 2: Normalized absorption (olive line) and phosphorescence (red line) spectra of **Re1–Re8** in deoxygenated toluene. Excitation wavelength was their respective absorption maxima.

Singlet Oxygen Generation

The appropriate photophysical properties, e.g., intense absorption in visible region and their long lived triplet states of the rhenium(I) complexes, **Re1-Re8** allowed us to examine the capability for photosensitization of singlet oxygen generation. Singlet oxygen quantum yields (Φ_Δ) were determined by comparing the intensity of the singlet oxygen phosphorescence peak at 1270 nm in the air-saturated solution with that of an optically matching reference sensitizer; tetraphenylporphyrin (TPP) was used as a standard (Φ_Δ^{TPP} = 0.66).[49] The values are presented in Table 3. As the result, all the complexes showed remarkably high values for Φ_Δ up to 0.99. These high $^1O_2$ generation quantum yields could be originated from the fact that the long lived triplet states (> 5 μs) of the photosensitizers facilitates the energy transfer (Dexter) to the dioxygen.[49] This is indeed the case with most of the rhenium dipyrrinates, particularly for **Re2** and **Re5**. The values Φ_Δ were found to be much better that the reported Re(I) phenanthroline and Ir(III) benzo[h]-quinoline complexes (Φ_Δ; 0.56 and 0.54 respectively.[46]

Furthermore, to confirm the singlet oxygen generation activity of the complexes, the photo-oxidation of 1,5-dihydroxynaphthalene (DHN) was investigated under the visible light irradiation (λ > 500 nm). In presence of the rhenium complexes, the photo-oxidation reaction effectively proceeded and the formation of oxygenated product, 5-hydroxy-1,4-naphthaquinone (Juglone)[50, 51] was monitored by optical spectrometry.

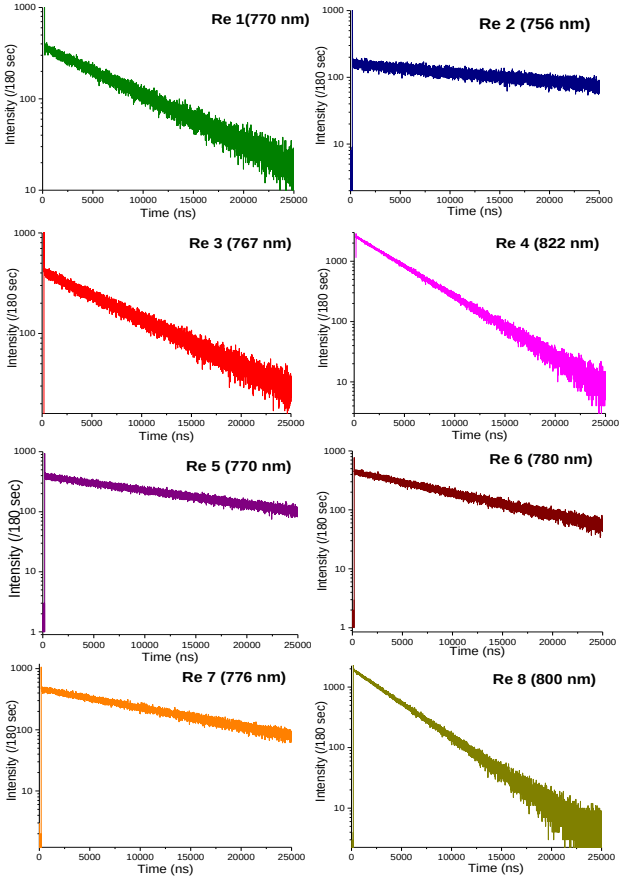

Figure 3. Phosphorescence decay profiles of **Re1–Re8** in deoxygenated toluene. All data collected at wavelength mentioned in the figure (λ_{ex} = 532 nm).

Table 3. Singlet oxygen quantum yield (Φ_Δ) and chemical yields of Juglone formed after 60 min.

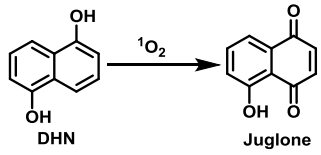

Sensitizer	Φ_Δ[b]	% Yield of Juglone after 60 min
Re1	0.89	87
Re2	0.98	77
Re3	0.82	86
Re4	0.74	99
Re5	0.99	94
Re6	0.75	95
Re7	0.79	97
Re8	0.81	99
None	--	4

The gradual decrease in the absorption peak of DHN at 301 nm, with the simultaneous appearance of a new peak at 427 nm, indicated formation of Juglone (Table 3).

The respective chemical yield of the product as a function of irradiation time for the photo-oxidation of DHN is given in Figure 4, which indicates that **Re4** showed the highest chemical yield for Juglone formation i.e., ≅ 99%. In contrast, in the absence of the sensitizers, the chemical yield of Juglone was only 4%, which suggests the rhenium complex is essential for this singlet oxygen generation under light.

According to the fact that the moderate singlet oxygen quantum yield of **Re4** showed the highest chemical yield of Juglone, we carried out the photochemical stability analysis of all the rhenium complexes. The absorption spectra of rhenium dipyrrinates were recorded upon irradiation by visible light (λ > 500 nm, Xe lamp 300W). From the analysis it was observed that, the molecule **Re4** was found to be a photochemically robust compound. In contrast, **Re2** with highest singlet oxygen generation quantum yield is getting degraded easily on irradiation (Figure 5). This result highlights that the good photostability of the sensitizers is crucial for practical applications, e.g., PDT.

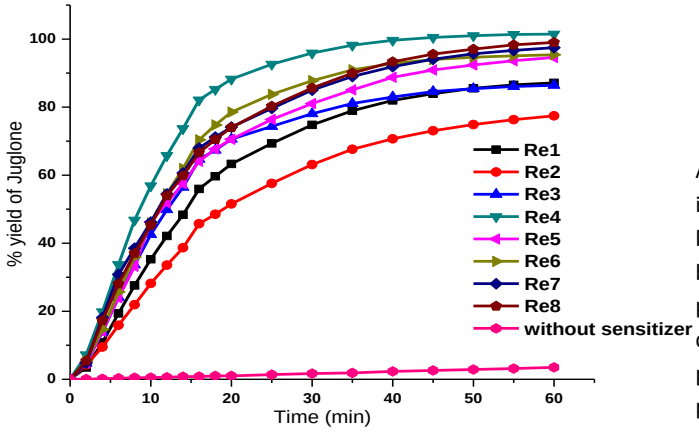

Figure 4. Plot of chemical yield as a function of irradiation time for the photo-oxidation of DHN using **Re1–Re8.**

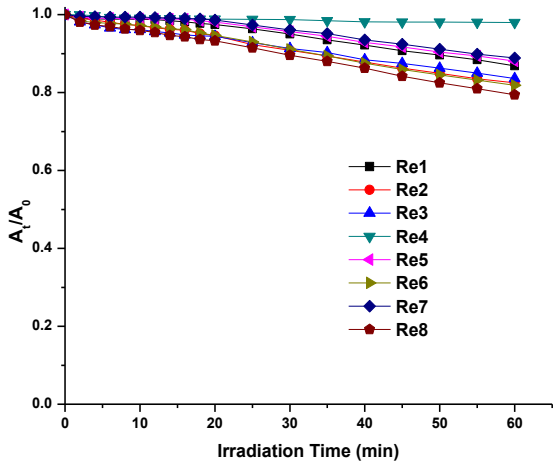

Figure 5. Plot of the change in absorption maxima of the Re complexes upon photoirradiation.

Electrochemical Studies

In order to understand the electrochemical properties of **Re1-Re8**, cyclic voltammetry studies were carried out in dry DCM containing 0.1 M tetrabutylammonium perchlorate (TBAP) as supporting electrolyte. The redox potential data and a comparison of reduction waves are summarised in Table 4 and Figure S70 (supplementary information, S38) respectively.

Table 4. Electrochemical redox data (V vs. SCE) of compounds **Re1–Re8** in DCM, containing 0.1 M TBAP as supporting electrolyte recorded at 50 mV/s scan speed and energy levels calculated from optical spectra.

Complex	$E1_{/2(ox)}$ [V] 1st	2nd	$E_{1/2(red)}$ [V]	HOMO [eV]	LUMO [eV]	ΔE [eV] (from CV)	ΔE [eV] (from Abs.)
Re1	0.34	0.95	–1.55	–4.76	–2.87	1.89	2.40
Re2	0.30	1.28	–1.52	–4.72	–2.90	1.82	2.41
Re3	0.34	0.95	–1.47	–4.76	–2.95	1.81	2.41
Re4	0.26	1.44	–1.28	–4.68	–3.14	1.54	2.34
Re5	0.42	1.43	–1.53	–4.84	–2.89	1.95	2.42
Re6	0.32	1.33	–1.41	–4.74	–3.01	1.73	2.40
Re7	0.31	1.35	–1.42	–4.73	–3.00	1.73	2.39
Re8	0.35	1.27	–1.33	–4.77	–3.09	1.68	2.36

All the complexes showed one quasi-reversible reduction and two irreversible oxidations; which are associated with the dipyrrin ligand. The oxidation and reduction potentials were thus affected by the presence of electron donating/withdrawing groups at the C5 position of the dipyrrin ligand. Complexes containing electron donating moieties, **Re1, Re2** and **Re3** exhibited first oxidation potential between 0.30 to 0.34 V (vs. SCE) and the second oxidation peak in the range of 0.95 to 1.28 V (Table 4). For complexes **Re4** to **Re8,** the first oxidation waves were observed between 0.26 to 0.42 V and the second oxidation peaks were in the range of 1.27 to 1.44 V (Table 4). Only one quasi-reversible reduction potentials were observed in cyclic voltammetry; and the reduction potentials of **Re4-Re8** were found in the range of –1.28 to –1.53 V. Among the eight rhenium dipyrrinates reported here, the higher value of first oxidation potential at 0.42 V was found in case of **Re5** having *p*-fluorophenyl moiety. The irreversible responses and similar values of the oxidation potentials of all the rhenium dipyrrinates suggested that the oxidation is associated with dipyrrin ligand.[52, 53] Typically, the reported rhenium mixed ligand complexes showed metal-centred oxidation waves between 1.59 to 1.63 eV.[38] However, the metal complexes **Re1–Re8** showed mainly dipyrrin centric electrochemistry including one electron redox processes which is consistent with the literature reports.[54, 55]

On this basis, the HOMO-LUMO energy gaps were determined by using measured redox potentials (Table 4). Likewise, the optical band gap[56] was calculated for compounds **Re1–Re8** from the absorption data (Table 4). The energetic stabilization for the LUMOs was slightly more in the compounds **Re4** and **Re8** than

the rest of the rhenium dipyrrinates**.** On the other hand, the HOMO of compound **Re5** was slightly lower in energy as compared to the other rhenium dipyrrinates. The HOMO-LUMO gap *ΔE* was highest for compound **Re5** among all rhenium dipyrrinates; the pattern of electrical band gap of **Re1**–**Re8** obtained from CV measurements correlated with the observed values of optical band gap (Table 4). The optical band gap for **Re2**, **Re3** and **Re5** were slightly higher than the other compounds. According to electrochemical data, compound **Re4** having a narrowest band gap, should have the most red-shifted absorption (*vide supra*). Indeed, this is the case and these electrochemical studies corroborate with the optical measurements. The lowest optical bandgap was observed for **Re4** among all the compounds; indicating that a pentafluorophenyl ring at C5-position has maximum effect on the electronic spectra of the compound.

Theoretical Calculations

Rhenium metal complexes, **Re1**–**Re8** was subjected to full geometry optimization by DFT-D3 methods using the Gaussian 09 program suite. The structural parameters of optimized geometries of the ground state **Re1**–**Re8** are incorporated in Table 5. The gas phase optimized geometrical structures of all the rhenium dipyrrinates in ground state are shown in supplementary information. In the optimized structures, the aryl substituents are non-coplanar with the dipyrrin core. The rhenium atom has distorted octahedral geometry with the two carbonyl group arranged in *trans* fashion w.r.t. dipyrrin core. The calculated metal–ligand bond distances in the optimized structure of all metal complexes are comparable (±0.05 Å) to those observed in the crystal structures. The marginal deviations in bond length data suggest good agreement between the molecule structures obtained by DFT and X-ray crystallography.

As depicted in Figure 6, there is a clear difference between the electron-rich derivatives, **Re1** and **Re3** and the others, **Re2**, **Re4**-**Re8**. The electron densities of **Re1** and **Re3** in HOMO are mainly spread on the C5 substituents; and those of LUMOs are localized on the dipyrrin core. In rest of the complexes **Re2**, **Re4**–**Re8**, the HOMOs consist of dipyrrin unit only; and the LUMOs are distributed between dipyrrin ligand and C5 substituents. Therefore, the complexes **Re1** and **Re3** may have intramolecular CT character, though the corresponding optical bands were negligibly observed. The DFT calculated LUMO energy level of **Re4** is slightly lower than those of other rhenium complexes, which is reflected in the lower reduction potential of the compounds measured by cyclic voltammetry (Table 4 and Figure 6). The experimentally obtained electrical and optical band gap harmonized with the calculated band gap of **Re2** and **Re5**, which showed slightly higher HOMO-LUMO gap as compared to other Re-dipyrrinates. Also, for other rhenium dipyrrinates the trend of HOMO-LUMO band gap, calculated by DFT is rather similar to the one obtained by cyclic voltammetry technique (Table 4).

Table 5. Calculated bond angles and lengths of optimized structures of **Re1-Re8.**

Complex	Bond Angles (°)	Bond Distances (Å)	
Re1	N1-Re-N2 83.43	Re-P1 2.558	Re-C46 1.942
		Re-N1 2.205	Re-C47 1.961
		Re-N2 2.199	Re-C48 1.943
Re2	N1-Re-N2 83.37	Re-P1 2.555	Re-C46 1.942
		Re-N1 2.198	Re-C47 1.943
		Re-N2 2.204	Re-C48 1.961
Re3	N1-Re-N2 83.31	Re-P1 2.557	Re-C44 1.942
		Re-N1 2.199	Re-C45 1.942
		Re-N2 2.206	Re-C46 1.961
Re4	N1-Re-N2 84.41	Re-P1 2.532	Re-C34 1.939
		Re-N1 2.206	Re-C35 1.969
		Re-N2 2.207	Re-C36 1.943
Re5	N1–Re–N2 83.46	Re–P1 2.563	Re–C34 1.942
		Re–N1 2.207	Re–C35 1.943
		Re–N2 2.200	Re–C36 1.959
Re6	N1–Re–N2 83.55	Re–P1 2.563	Re–C34 1.943
		Re–N1 2.201	Re–C35 1.942
		Re–N2 2.206	Re–C36 1.959
Re7	N1–Re–N2 83.44	Re–P1 2.558	Re–C34 1.943
		Re–N1 2.204	Re–C35 1.961
		Re–N2 2.201	Re–C36 1.943
Re8	N1–Re–N2 83.32	Re–P1 2.551	Re–C46 1.962
		Re–N1 2.206	Re–C47 1.942
		Re–N2 2.201	Re–C48 1.942

The vertical excitation energies of the lowest 10 excited singlet states of **Re1-Re8** were calculated by TDDFT method at the B3LYP level with the 6-31G** basis set for non-metals and the SDD basis set for Re atom in toluene and are given in supplementary information. The calculated absorption maxima are blue shifted as compared to the experimentally observed values; the consistent underestimation of λ_{max} for all the molecules is due to the inherent limitations of vertical approximation. The most intense calculated singlet transition for **Re1** was observed from $S_0 \rightarrow S_2$. In the electronic transition of **Re2** major contribution is from H-3 → LUMO (40%) and HOMO → LUMO (51%). Major electronic transition in **Re3** is from $S_0 \rightarrow S_2$. In the case of **Re4-Re8**, the most intense singlet transition was observed from $S_0 \rightarrow S_1$. The calculated absorption maxima of **Re4** and **Re8** were red shifted as compared to other molecules. This trend is exactly matching with the experimental absorption data. Along with the singlet excited state calculations, we calculated the triplet state energies using the same level of

parameters. The energies were comparable with the experimental data (supplementary information S48).

Figure 6. DFT calculated frontier orbitals and their HOMO/LUMO energies of **Re1–Re8.**

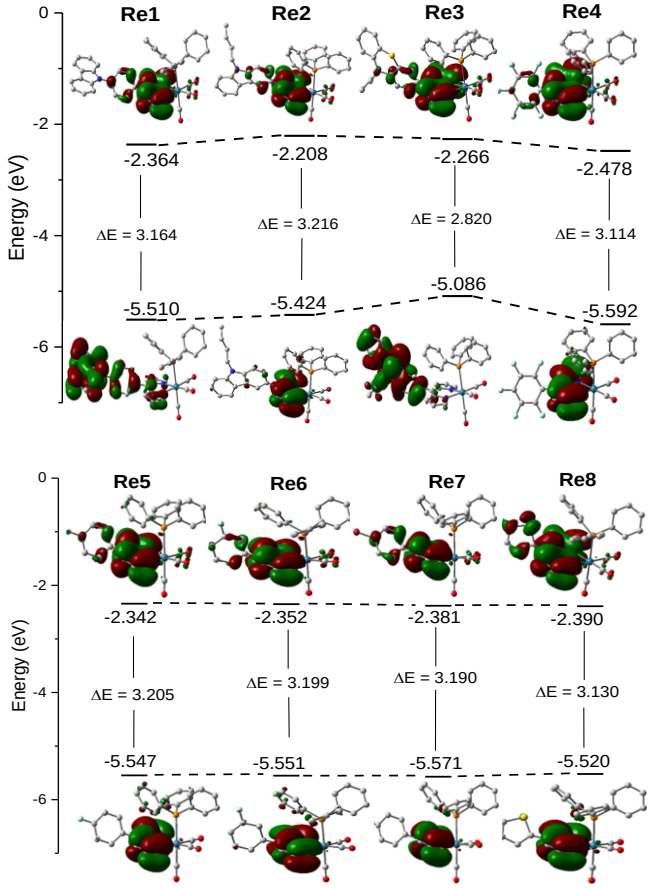

Conclusion

In summary, a series of rhenium dipyrrinates comprising variety of aromatic C5 substituents have been synthesized and characterized. The absorption maxima were red shifted (12 nm) for rhenium dipyrrinates having pentafluorophenyl (**Re4**) and thienyl (**Re8**) groups. Upon excitation at their respective absorption maxima, moderate phosphorescence was observed at room temperature in between 681 to 736 nm. Large Stokes shifts (from 5682 to 6957 cm^{-1}) were observed for all the complexes. The phosphorescence lifetimes of the complexes are varied by the substituents in the micro-second order, and these long-lived triplet rhenium dipyrrinates are capable of sensitizing for efficient singlet oxygen generation (Φ_Δ : 75–99%). In part, electron-deficient substituents in the photosensitizers (e.g., **Re4**) may play a role in the photostability as inferred from the lowering HOMO energies observed in the electrochemical study. These observed spectral features were well interpreted by the dispersion-corrected DFT calculations. Therefore, the current photosensitizers prepared in this work would serve as potential PDT agents for biological treatment. Further investigation of the modified dipyrrinato metal complexes is underway in our laboratory.

View Article Online
DOI: 10.1039/C8DT04540B

Conflicts of interest

There are no conflicts to declare.

Acknowledgements

Financial support from SERB (EMR/2015/000779) Govt. of India, is greatly acknowledged. NM and PK thank IIT Gandhinagar for fellowship and infrastructural support. Part of this work in Japan was supported by Grants-in-Aid (JP15K13646 to HF, JP16K05700, and JP17H05377 to MI) from Japan Society for the Promotion of Science (JSPS).

Supporting Information

The characterization data like Mass, ^{1}H, ^{13}C, ^{31}P and ^{19}F NMR spectra; 2D-COSY NMR spectra for selected compounds are provided. The DFT optimized structures of the compounds **Re1–Re8** are available. Also, the total energy and coordinates used for DFT calculations of compounds **Re1–Re8** are shown. The corresponding CIF files of compounds **Re1** and **Re3–Re7** are provided separately.

Experimental

Instrumentation and Reagents

Unless otherwise mentioned, all the reagents and solvents were purchased from Aldrich, Acros Organics or Merck and used without further purification. Pyrrole was distilled under vacuum prior to use. Neutral Alumina (Brockman Grade I–II) and silica gel (60–120 mesh size) were used for column chromatography. The NMR spectra of compounds were recorded with Bruker Avance III 500 MHz NMR spectrometer. ESI-MS spectra of compounds were recorded on Water Synapt–G2S ESI-Q-OTF mass instrument. MALDI mass data of compounds were recorded on Bruker Daltonics MALDI-TOF instrument. IR spectra of samples were recorded on Perkin Elmer L1600300 Spectrum TWO LITA. Absorption spectra were recorded with UV-1700 (Shimadzu, Japan). Phosphorescence spectra and absolute quantum yields of emission were measured with phosphorescence quantum yield measurement system (C9920-02, Hamamatsu). Cyclic voltammetry (CV) studies were carried out with an electrochemical system (CH1660E, CH instruments, USA) utilizing the three electrode configuration consisting of a glassy carbon (working electrode), platinum wire (auxiliary electrode) and saturated calomel (reference electrode) electrodes. The experiments were done under nitrogen atmosphere in dry DCM using 0.1 M *n*-tetrabutylammonium perchlorate as supporting electrolyte. All potentials were calibrated vs. saturated calomel electrode by the addition of ferrocene as an internal standard, taking $E_{½}$ (Fc/Fc^{+}) = 0.38 V *vs.* SCE.

Computational Methodology

Each metal complex structure **Re1–Re8** was subjected to full geometry optimization by DFT-D3 methods[57] using the Gaussian 09 program at the Becke's three parameter exact-functional combined with gradient-corrected correlational functional of Lee, Yang and Parr (B3LYP)[58, 59] level with the 6-31G** basis set for non-metals and the SDD[60] basis set for rhenium atom. The crystal data for six molecules are available, thus X-ray crystal structures were used for geometry optimization without symmetry restrictions. All the Density functional theory (DFT) calculations were performed using Gaussian 09 molecular modelling software.[61] The solvent was described by CPCM.[62] Low-lying singlet and triplet excited states at the ground-state geometry were calculated by TDDFT.[63] For visualization of the optimized geometries and the molecular orbitals, GaussView[64] software was used.

Singlet Oxygen Quantum Yield

For the Singlet oxygen quantum yield calculation, an air saturated solution of complexes in a quartz cell was excited at 512 nm using a HORIBA SPEX Fluorolog-NIR at room temperature. The generation of singlet oxygen was monitored at 1270 nm and the quantum yields were determined by relative quantum yield calculation method using tetraphenylporphyrin (Φ_{Δ}^{TPP} = 0.66) as a standard.

Catalytic Reaction

To analyze the catalytic activity of the complexes, a oxygen saturated CH_2Cl_2: MeOH (9:1) solution containing 1,5-dihydroxynaphthalene (DHN) (3.6 X 10^{-4} M) and a sensitizer (10 mol% vs DHN) was place into a 10 mm width quartz cell. Then the solution was irradiated using Xenon lamp (Asahi Spectra, MAX301, 300 W, through band pass filter at 500 nm). UV-vis absorption spectra were recorded at the intervals of 2-10 min on a UV-3150PC spectrometer. The progress of the reaction was monitored by decrease in the absorption peak of DHN at 301 nm with the appearance of a new peak at 427 nm, typical for Juglone. The concentration of DHN and Juglone was calculated by using molar extinction coefficients. (ε_{DHN} = 7240; $\varepsilon_{Juglone}$ = 3370).

Photostability

3.6 X 10^{-4} M solution of Re-complexes in CH_2Cl_2: MeOH (9:1) was placed into a quartz cell with path length 10 mm and oxygen was bubbled for 10 min. The solution was then irradiated using visible light (> 500 nm). Absorption spectra of these samples were recorded at intervals of 2-10 min.

General Synthesis of Dipyrrins

Dipyrromethanes[22] (300.00 mg, 0.77 mmol) dissolved in dry DCM (21.00 mL) and solution of *p*-chloranil (265.47 mg, 1.08 mmol) in dry DCM (4.10 mL) was added drop wise and then allowed to oxidize at room temperature with continuous stirring for 19 h. Column chromatography was carried out on neutral alumina using DCM/ hexane mixture.

Compound 1: General synthesis was performed. The desired compound was purified by neutral alumina column using 90% DCM/hexane mixture. Yield: (192.00 mg, 64%); m.p. 178 °C; IR (neat, cm^{-1}): 2920, 2848, 1565, 1513, 1450, 1387, 1224, 1009, 804, 740, 720, 604; ^{1}H NMR (500 MHz, $CDCl_3$, δ ppm): 8.17 (d, *J* = 8Hz, 2H, Ar-*H*), 7.75 (dd, *J* = 2Hz, 2H, Ar-*H*), 7.69 (m, 4H, α-pyrrolic-*H* and Ar-*H*), 7.54 (d, *J* = 8Hz, 2H, Ar-*H*), 7.46 (m, 2H, Ar-*H*), 7.33 (m, 2H, Ar-*H*), 6.76 (d, *J* = 4Hz, 2H, β-pyrrolic-*H*), 6.47 (m, 2H, β-pyrrolic-*H*); ^{13}C NMR (125.7 MHz, $CDCl_3$, δ ppm): 143.9, 140.6, 138.5, 136.2, 132.3, 128.9, 126.1, 125.9, 123.6, 120.4, 120.2, 117.8, 109.7, 30.8; ESI-MS: $C_{27}H_{20}N_3^+$ $[M+H]^+$: calcd *m/z* 386.1657, found *m/z* 386.1544.

Compound 2: General synthesis was followed. The desired compound was purified by neutral alumina column using 90% DCM/hexane mixture. Yield: (108.00 mg, 38%); m.p. 150 °C; IR (neat, cm^{-1}): 2923, 2848, 1555, 1466, 1380, 1355, 1330, 1245, 1211, 1120, 1005, 880, 800, 745, 720; ^{1}H NMR (500 MHz, $CDCl_3$, δ ppm): 8.25 (s, 1H, Ar-*H*), 8.09 (d, *J* = 8Hz, 1H, Ar-*H*), 7.67 (s, 2H, α-pyrrolic-*H*), 7.63 (d, *J* = 8Hz, 1H, Ar-*H*), 7.49 (d, *J* =7.5 Hz, 1H, Ar-*H*), 7.45 (m, 2H, Ar-*H*), 7.26 (d, *J* = 7Hz, 1H, Ar-*H*), 6.70 (d, *J* = 4 Hz, 2H, β-pyrrolic-*H*), 6.42 (d, *J* = 3.5 Hz, 2H, β-pyrrolic-*H*), 4.36 (t, *J* = 7Hz, 2H, N-C*H*$_2$-C-), 1.92 (m, 2H, -C-C*H*$_2$-C-), 1.48 (m, 2H, -C-C*H*$_2$-CH$_3$), 0.99 (t, *J* = 7 Hz, 3H, -C-C*H*$_3$); ^{13}C NMR (125.7 MHz, $CDCl_3$, δ ppm): 143.6, 142.9, 141.3, 140.9, 129.36, 129.1, 128.0, 126.1, 123.4, 122.7, 122.2, 120.5, 119.3, 117.3, 108.9, 107.6, 43.1, 31.1, 20.6, 13.8; ESI-MS: $C_{25}H_{24}N_3^+$ $[M+H]^+$: calcd *m/z* 366.1970, found *m/z* 366.1868.

Compound 3: General synthesis was followed. The desired compound was purified by neutral alumina column using 70% DCM/hexane mixture. Yield: (122.30 mg, 41%); m.p. 79 °C; IR (neat, cm^{-1}): 2921, 2850, 1564, 1460, 1380, 1350, 1246, 1120, 1095, 1041, 1005, 960, 805, 745, 720, 595; ^{1}H NMR (500 MHz, $CDCl_3$, δ ppm): 7.62 (s, 2H, α-pyrrolic-*H*), 7.283 (m, 2H, Ar-*H*), 7.15 (m, 2H, Ar-*H*), 6.92 (m, 3H, Ar-*H*), 6.68 (d, *J* = 4 Hz, 2H, β-pyrrolic-*H*), 6.39 (m, 2H, β-pyrrolic-*H*), 3.90 (t, *J* = 7 Hz, 2H, N-C*H*$_2$-C-), 1.85 (m, 2H, -C-C*H*$_2$-C-), 1.50 (m, 2H, -C-C*H*$_2$-CH$_3$), 0.98 (t, *J* = 7 Hz, 3H, -C-C*H*$_3$); ^{13}C NMR (125.7 MHz, $CDCl_3$, δ ppm): 146.2, 144.6, 143.3, 141.1, 140.8, 131.4, 130.4, 129.7, 128.6, 127.5, 127.3, 124.4, 124.1, 122.7, 117.4, 115.5, 114.2, 47.3, 29.1, 20.2, 13.8; ESI-MS: $C_{25}H_{24}N_3S^+$ $[M+H]^+$: calcd *m/z* 398.1691, found *m/z* 398.1661.

Compound 4: General synthesis was followed. The desired compound was purified by neutral alumina column using 30% DCM/hexane mixture. Yield: (135.00 mg, 45%); m.p. 153 °C; IR (neat, cm^{-1}): 2921, 2855, 1585, 1644, 1520, 1495, 1380, 1350, 1115, 1075, 990, 820, 760, 745, 600, 570; ^{1}H NMR (500 MHz, $CDCl_3$, δ ppm): 7.65 (s, 2H, α-pyrrolic-*H*), 6.47 (d, *J* = 4.5 Hz, 2H, β-pyrrolic-*H*), 6.42 (d, *J* = 4 Hz, 2H, β-pyrrolic-*H*); ^{13}C NMR (125.7 MHz, $CDCl_3$, δ ppm): 145.3, 140.3, 126.9, 123.9, 118.9; ESI-MS: $C_{15}H_8F_5N_2^+$ $[M+H]^+$: calcd *m/z* 311.0608, found *m/z* 311.0500.

Compound 5: General synthesis was performed. The desired compound was purified by neutral alumina column using 90% DCM/hexane mixture. Yield: (157.00 mg, 32%); m.p. 146 °C; IR

(neat, cm^{-1}): 2918, 2850, 1600, 1560, 1505, 1410, 1331, 1225, 1160, 1090, 1045, 975, 810, 775, 726, 560; ^{1}H NMR (500 MHz, $CDCl_3$, δ ppm): 7.63 (s, 2H, α-pyrrolic-*H*), 7.47 (dd, *J* = 3, 5.5 Hz, 2H, Ar-*H*), 7.13 (m, 2H, Ar-*H*), 6.56 (d, *J* = 4 Hz, 2H, β-pyrrolic-*H*), 6.39 (dd, *J* = 1, 3.5 Hz, 2H, β-pyrrolic-*H*); ^{13}C NMR (125.7 MHz, $CDCl_3$, δ ppm): 143.7, 140.9, 140.6, 133.3, 132.5, 132.5, 128.5, 117.7, 114.8, 114.6; ESI-MS: $C_{15}H_{12}FN_2^+$ $[M+H]^+$: calcd *m/z* 239.0985, found *m/z* 239.0911.

Compound 6: General synthesis was performed. The desired compound was purified by neutral alumina column using 40% DCM/hexane mixture. Yield: (107.00 mg, 36%); m.p. 94 °C; IR (neat, cm^{-1}): 2931, 2857, 1610, 1585, 1565, 1485, 1385, 1228, 1119, 1095, 1005, 1045, 880, 775, 719, 520; ^{1}H NMR (500 MHz, $CDCl_3$, δ ppm): 7.65 (s, 2H, α-pyrrolic-*H*), 7.41 (d, *J* = 7 Hz, 1H, Ar-*H*), 7.27 (d, *J* = 8 Hz, 1H, Ar-*H*), 7.21 (m, 2H, Ar-*H*), 6.58 (d, *J* = 4 Hz, 2H, β-pyrrolic-*H*), 6.40 (d, *J* = 4Hz, 2H, β-pyrrolic-*H*); ^{13}C NMR (125.7 MHz, $CDCl_3$, δ ppm): 143.9, 140.6, 140.1, 139.4, 129.1, 128.5, 126.5, 117.8, 117.7, 117.6, 115.8, 115.7; ESI-MS: $C_{15}H_{12}FN_2^+$ $[M+H]^+$: calcd *m/z* 239.0985, found *m/z* 239.0911.

Compound 7: General synthesis was performed. The desired compound was purified by neutral alumina column using 0.1% methanol/DCM mixture. Yield: (218.00 mg, 73%); m.p. 151 °C; IR (neat, cm^{-1}): 2921, 2847, 1568, 1485, 1382, 1329, 1264, 1176, 1120, 1045, 1010, 935, 875, 795, 775, 720, 515; ^{1}H NMR (500 MHz, $CDCl_3$, δ ppm): 7.6 (s, 2H, α-pyrrolic-*H*), 7.59 (d, *J* = 8 Hz, 2H, Ar-*H*), 7.37 (d, *J* = 8 Hz, 2H, Ar-*H*), 6.56 (d, *J* = 4 Hz, 2H, β-pyrrolic-*H*), 6.41 (d, *J* = 4 Hz, 2H, β-pyrrolic-*H*); ^{13}C NMR (125.7 MHz, $CDCl_3$, δ ppm): 143.9, 140.6, 140.3, 136.2, 132.3, 130.9, 128.8, 123.4, 117.8; ESI-MS: $C_{15}H_{12}BrN_2^+$ $[M+H]^+$: calcd *m/z* 299.0184, found *m/z* 299.0103.

Compound 8: General synthesis was followed. The desired compound was purified by neutral alumina column using 50% DCM/hexane mixture. Yield: (177.00 mg, 59%); m.p. 128 °C; IR (neat, cm^{-1}): 2921, 2850, 1547, 1379, 1338, 1225, 1115, 1090, 1039, 985, 789, 702, 540, 460; ^{1}H NMR (500 MHz, $CDCl_3$, δ ppm): 7.64 (s, 2H, α-pyrrolic-*H*), 7.54 (d, *J* = 5 Hz, 1H, Ar-*H*), 7.37 (d, *J* = 3.5 Hz, 1H, Ar-*H*), 7.160 (t, *J* = 4 Hz, 1H, Ar-*H*), 6.95 (d, *J* = 4 Hz, 2H, β-pyrrolic-*H*), 6.43 (d, *J* = 4 Hz, 2H, β-pyrrolic-*H*); ^{13}C NMR (125.7 MHz, $CDCl_3$, δ ppm): 143.7, 140.6, 138.1, 131.7, 128.9, 128.7, 126.9, 117.7, 108.4; ESI-MS: $C_{13}H_{11}N_2S^+$ $[M+H]^+$: calcd *m/z* 227.0643, found *m/z* 227.0562.

General Synthesis of Re(I) Dipyrrinato Complexes

In a 100 mL round bottom flask, $Re(CO)_5Cl$ (1 equiv.) and dipyrrin (1 equiv.) were dissolved in dry toluene (1.61 mL) and allowed to reflux at about 100 °C under inert atmosphere. At 100 °C triethylamine (2 equiv.) was added and heating continued for 1 h, then added triphenylphosphine (1 equiv.) and reaction mixture allowed to heat for another 1 h. Reaction progress was monitored by TLC, the initial dipyrrin spot vanishes and two new spots observed. All volatiles were removed under rotary evaporator before purifying by column chromatography. Then column chromatography on neutral alumina was performed using (10–15%) DCM/ hexane as eluent.

Compound Re1: General synthesis was followed. The desired compound was purified by neutral alumina column using 20% DCM/hexane mixture. Yield: (66.00 mg, 88%); m.p. 191 °C; IR (neat, cm^{-1}): 2923, 2852, 2020 (CO), 1926 (CO), 1896 (CO), 1604, 1548, 1495, 1452, 1379, 1242, 1033, 995, 726, 693; ^{1}H NMR (500 MHz, $CDCl_3$, δ ppm): 8.17 (d, *J* = 7.5 Hz, 2H, Ar-*H*), 7.75 (s, 2H, α-pyrrolic-*H*), 7.60 (m, 2H, Ar-*H*), 7.5 (m, 5H, Ar-*H*), 7.34 (m, 5H, Ar-*H*), 7.26 (m, 6H, Ar-*H*), 6.95 (m, 6H, Ar-*H*), 6.73 (d, *J* = 8 Hz, 1H, Ar-*H*), 6.55 (d, *J* = 4 Hz, 2H, β-pyrrolic-*H*), 6.37 (d, *J* = 4 Hz, 2H, β-pyrrolic-*H*); ^{13}C NMR (125.7 MHz, $CDCl_3$, δ ppm): 196.3, 154.5, 146.7, 140.7, 137.6, 136.6, 133.5, 133.5, 131.7, 131.2, 130.9, 130.6, 130.0, 128.4, 128.3, 126.0, 125.6, 125.2, 123.5, 120.4, 120.2, 118.9, 109.7; ^{31}P NMR (202.4 MHz, $CDCl_3$, δ ppm): 11.40; ESI-MS: $C_{48}H_{34}N_3O_3PRe^+$ $[M+H]^+$: calcd *m/z* 918.1895, found *m/z* 918.1787.

Compound Re2: General synthesis was followed. The desired compound was purified by neutral alumina column using 15% DCM/hexane mixture. Yield: (63.12 mg, 86%); m.p. 171 °C; IR (neat, cm^{-1}): 2918, 2849, 2016 (CO), 1920 (CO), 1891 (CO), 1602, 1543, 1379, 1342, 1241, 1035, 995, 727, 694; ^{1}H NMR (500 MHz, $CDCl_3$, δ ppm): 8.12 (s, 1H, Ar-*H*), 8.03 (d, *J* = 7.5 Hz, 1H, Ar-*H*), 7.71 (d, *J* = 15 Hz, 2H, α-pyrrolic-*H*), 7.50-7.35 (m, 7H, Ar-*H*), 7.25 (m, 5H, Ar-*H*), 7.11 (s, 1H, Ar-*H*), 6.96 (m, 6H, Ar-*H*), 6.65 (d, *J* = 7.5 Hz, 1H, Ar-*H*), 6.47 (s, 2H, β-pyrrolic-*H*), 6.29 (d, *J* = 6 Hz, 2H, β-pyrrolic-*H*), 4.34 (t, *J* = 7Hz, 2H, N-CH_2-C-), 1.92 (m, 2H, -C-CH_2-C-), 1.48 (m, 2H, -C-CH_2-CH_3), 0.99 (t, *J* = 7Hz, 3H, -C-CH_3); ^{13}C NMR (125.7 MHz, $CDCl_3$, δ ppm): 196.5, 153.8, 140.9, 140.2, 137.5, 133.6, 133.5, 132.3, 132.3, 131.0, 130.7, 129.9, 129.3,128.4, 128.3, 125.9, 122.6, 122.5, 122.6, 122.5, 122.1, 119.0, 118.4, 109.0, 107.0, 43.1, 31.2, 20.6, 13.9; ^{31}P NMR (202.4 MHz, $CDCl_3$, δ ppm): 10.68; MALDI-MS: $C_{46}H_{38}N_3O_3PRe^+$ $[M+H]^+$: calcd *m/z* 898.0088, found *m/z* 898.440.

Compound Re3: General synthesis was followed. The desired compound was purified by neutral alumina column using 18% DCM/ hexane mixture. Yield: (45.20 mg, 71%); m.p. 163 °C; IR (neat, cm^{-1}): 2919, 2855, 2016 (CO), 1923 (CO), 1890 (CO), 1602, 1544, 1463, 1379, 1341, 1242, 1034, 994, 747, 695; ^{1}H NMR (500 MHz, $CDCl_3$, δ ppm): 7.70 (bs, 2H, α-pyrrolic-*H*), 7.35 (m, 3H, Ar-*H*), 7.19 (m, 8H, Ar-*H*), 6.92 (m, 7H, Ar-*H*), 6.81 (d, *J* = 8 Hz, 1H, Ar-*H*), 6.72 (d, *J* = 6.5 Hz, 1H, Ar-*H*), 6.50 (d, *J* = 4 Hz, 2H, β-pyrrolic-*H*), 6.34 (d, *J* = 7.5 Hz, 1H, Ar-*H*), 6.30 (bs, 2H, β-pyrrolic-*H*), 6.10 (s, 1H, Ar-*H*), 3.88 (t, *J* = 7 Hz, 2H, N-CH_2-C-), 1.84 (m, 2H, -C-CH_2-C-), 1.47 (m, 2H, -C-CH_2-CH_3), 0.98 (t, *J* = 7 Hz, 3H, -C-CH_3); ^{13}C NMR (125.7 MHz, $CDCl_3$, δ ppm): 196.5, 196.4, 190.20, 154.2, 154.1, 147.1, 145.2, 144.8, 136.7, 133.5, 133.4, 131.8, 130.8, 130.4, 130.0, 129.8, 129.3, 128.7, 128.4, 128.3, 127.5, 127.4, 124.4, 122.5, 118.5, 115.5, 113.6, 47.3, 29.1, 20.3, 13.8; ^{31}P NMR (202.4 MHz, $CDCl_3$, δ ppm): 10.76; MALDI-MS: $C_{46}H_{38}N_3O_3PReS^+$ $[M+H]^+$: calcd *m/z* 930.1929, found *m/z* 930.706.

Compound Re4: General synthesis was followed. The desired compound was purified by neutral alumina column using 10% DCM/hexane mixture. Yield: (72.08 mg, 88%); m.p. 183 °C; IR (neat, cm^{-1}): 2926, 2893, 2021 (CO), 1926 (CO), 1891 (CO), 1655, 1561, 1498, 1381, 1343, 1243, 1033, 989, 888, 751, 694; ^{1}H NMR (500 MHz, $CDCl_3$, δ ppm): 7.48 (s, 2H, α-pyrrolic-*H*), 7.31 (d, *J* = 7 Hz, 3H, Ar-*H*), 7.22 (m, 5H, Ar-*H*), 7.08 (m, 7H, Ar-*H*), 6.38 (d, *J* = 4 Hz, 2H, β-pyrrolic-*H*), 6.20 (d, *J* = 4.5 Hz, 2H, β-pyrrolic-*H*); ^{13}C NMR (125.7 MHz, $CDCl_3$, δ ppm): 196.3, 189.4, 188.8, 155.7, 145.7, 135.4, 133.5, 133.4, 130.7, 130.3, 129.9, 129.6, 128.4, 128.3, 120.0, 113.4, 113.2, 113.0; ^{31}P NMR (202.4 MHz, $CDCl_3$, δ ppm): 15.84; ESI-MS: $C_{36}H_{22}F_5N_2O_3PRe^+$ $[M+H]^+$: calcd *m/z* 843.0846, found *m/z* 843.0773.

Compound Re5: General synthesis was followed. The desired compound was purified by neutral alumina column using 8 % DCM/hexane mixture. Yield: (69.00 mg, 71%); m.p. 168 °C; IR (neat, cm^{-1}): 2921, 2850, 2017 (CO), 1922 (CO), 1893 (CO), 1607, 1547, 1380, 1341, 1241, 1034, 994, 816, 730, 695; ^{1}H NMR (500 MHz, $CDCl_3$, δ ppm): 7.70 (d, *J* = 1 Hz, 2H, α-pyrrolic-*H*), 7.33 (m, 4H, Ar-*H*), 7.22 (m, 6H, Ar-*H*), 7.05 (m, 1H, Ar-*H*), 6.932 (m, 1H, Ar-*H*), 6.90 (m, 6H, Ar-*H*), 6.47 (m, 1H, Ar-*H*), 6.37 (d, *J* = 4.5 Hz, 2H, β-pyrrolic-*H*), 6.30 (m, 2H, β-pyrrolic-*H*); ^{13}C NMR (125.7 MHz, $CDCl_3$, δ ppm): 196.3, 189.4, 163.6, 161.6, 154.4, 154.4, 146.6, 136.7, 134.5, 134.5, 133.5, 133.4, 131.9, 131.8, 131.6, 131.4, 131.3, 130.9, 130.5, 129.9, 129.9, 128.4, 128.3, 118.7, 114.2, 114.0, 113.9, 113.7; ^{31}P NMR (202.4 MHz, $CDCl_3$, δ ppm): 11.27; ESI-MS: $C_{36}H_{26}FN_2O_3PRe^+$ $[M+H]^+$: calcd *m/z* 771.1223, found *m/z* 771.1191.

Compound Re6: General synthesis was followed. The desired compound was purified by neutral alumina column using 10% DCM/hexane mixture. Yield: (55.10 mg, 57%); m.p. 186 °C; IR (neat, cm^{-1}): 2920, 2857, 2018 (CO), 1924 (CO), 1892 (CO), 1612, 1547, 1379, 1342, 1245, 1034, 993, 812, 723, 694; ^{1}H NMR (500 MHz, $CDCl_3$, δ ppm): 7.71 (d, *J* = 9.5 Hz, 2H, α-pyrrolic-*H*), 7.33 (m, 4H, Ar-*H*), 7.24 (m, 6H, Ar-*H*), 7.16 (m, 1H, Ar-*H*), 7.11 (m, 1H, Ar-*H*), 6.92 (m, 6H, Ar-*H*), 6.39 (s, 2H, β-pyrrolic-*H*), 6.31 (s, 2H, β-pyrrolic-*H*), 6.17 (d, *J* = 9.5 Hz, 1H, Ar-*H*); ^{13}C NMR (125.7 MHz, $CDCl_3$, δ ppm):196.3, 190.0, 189.4, 162.4, 160.4, 154.5, 145.9, 140.5, 136.2, 130.8, 130.4, 130.0, 128.3, 126.0, 126.0, 125.5, 118.9, 117.5, 117.3, 117.1, 116.8, 114.9, 114.8; ^{31}P NMR (202.4 MHz, $CDCl_3$, δ ppm): 11.27; ESI-MS: $C_{36}H_{26}FN_2O_2PRe^+$ $[M+H]^+$: calcd *m/z* 771.1223, found *m/z* 771.1191.

Compound Re7: General synthesis was followed. The desired compound was purified by neutral alumina column using 8% DCM/hexane mixture. Yield: (46.32 mg, 55%); m.p. 182 °C; IR (neat, cm^{-1}): 2932, 2852, 2017 (CO), 1924 (CO), 1891 (CO), 1547, 1380, 1342, 1245, 1035, 994, 727, 694; ^{1}H NMR (500 MHz, DMSO-d_6, δ ppm): 7.69 (s, 2H, Ar-H, α-pyrrolic-*H*), 7.62 (m, 2H, Ar-*H*), 7.46 (m, 3H, Ar-*H*), 7.36 (m, 7H, Ar-*H*), 6.88 (t, *J* = 9 Hz, 6H, Ar-*H*), 6.52 (d, *J* = 7.5 Hz, 1H, Ar-*H*), 6.4 (d, *J* = 4 Hz, 2H, β-pyrrolic-*H*), 6.34 (d, *J* = 4.5 Hz, 2H, β-pyrrolic-*H*); ^{13}C NMR (125.7 MHz, DMSO-d_6, δ ppm): 196.3, 190.0, 189.4, 154.5, 146.2, 137.4, 136.3, 133.5, 133.4, 131.7, 131.6, 131.3, 130.8, 130.5, 130.3, 130.0, 129.9, 128.4, 128.3, 122.3, 118.9; ^{31}P NMR (202.4 MHz, $CDCl_3$, δ ppm): 10.66; MALDI-MS: $C_{36}H_{26}BrN_2O_3PRe^+$ $[M+H]^+$: calcd *m/z* 831.0422, found *m/z* 831.196.

Compound Re8: General synthesis was followed. The desired compound was purified by neutral alumina column using 10% DCM/hexane mixture. Yield: (45.03 mg, 45%); m.p. 174 °C; IR (neat, cm^{-1}): 2917, 2852, 2016 (CO), 1924 (CO), 1890 (CO), 1542, 1379, 1340, 1241, 1035, 993, 813, 721, 694; ^{1}H NMR (500 MHz, DMSO-d_6, δ ppm): 7.76 (d, *J* = 5 Hz, 1H, Ar-*H*), 7.67 (s, 2H, α-pyrrolic-*H*), 7.46 (m, 3H, Ar-*H*), 7.36 (m, 6H, Ar-*H*), 7.15 (m, 1H, Ar-*H*), 7.03 (s, 1H, Ar-*H*), 6.92 (t, *J* = 9 Hz, 6H, Ar-*H*), 6.66 (d, *J* = 4 Hz, 2H, β-pyrrolic-*H*), 6.39 (d, *J* = 4 Hz, 2H, β-pyrrolic-*H*); ^{13}C NMR (125.7 MHz, DMSO-d_6, δ ppm): 196.4, 189.4, 154.6, 140.1, 138.7, 137.0, 133.5, 133.4, 131.8, 130.8, 130.5, 130.1, 129.9, 128.4, 128.3, 126.4, 125.8, 118.7; ^{31}P NMR (202.4 MHz, $CDCl_3$, δ ppm): 12.14; MALDI-MS: $C_{34}H_{25}N_2O_3PReS^+$ $[M+H]^+$: calcd *m/z* 759.0881, found *m/z* 759.289.

References

1. J. K. Laha, S. Dhanalekshmi, M. Taniguchi, A. Ambroise and J. S. Lindsey**,** *Org. Process Res. Dev.***,** 2003, **7**, 799-812.
2. D. T. Gryko, D. Gryko and C.-H. Lee, *Chem. Soc. Rev.*, 2012, **41**, 3780-3789.
3. J. S. Lindsey, *Acc. Chem. Res.*, 2010, **43,** 300-311.
4. S. Das, H. R. Bhat, N. Balsukuri, P. C. Jha, Y. Hisamune, M. Ishida, H. Furuta, S. Mori and I. Gupta, *Inorg. Chem. Front.*, 2017, **4**, 618-638.
5. B. Koszarna and D. T. Gryko, *J. Org. Chem.*, 2006, **71**, 3707-3717.
6. T. Ito, Y. Hayashi, S. Shimizu, J. Y. Shin, N. Kobayashi and H. Shinokubo, *Angew. Chem. Int. Ed. Engl.*, 2012, **51**, 8542-8545.
7. H. Omori, S. Hiroto and H. Shinokubo, *Chem. Eur. J.*, 2017, **23**, 7866-7870.
8. T. E. Wood and A. Thompson, *Chem. Rev.*, 2007, **107**, 1831-1861.
9. S. Das and I. Gupta, *Inorg. Chem. Commun*., 2015, **60**, 54-60.
10. Q. Zhao, F. Li and C. Huang, *Chem. Soc. Rev.*, 2010, **39**, 3007-3030.
11. M. M. Ravikanth, L. Vellanki and R. Sharma, *Rep. Org. Chem.*, 2016, **6**, 1-24.
12. A. Loudet and K. Burgess, *Chem. Rev.*, 2007, **107**, 4891-4932.
13. N. Boens, V. Leen and W. Dehaen, *Chem. Soc. Rev.*, 2012, **41**, 1130-1172.
14. P. E. Kesavan, S. Das, M. Y. Lone, P. C. Jha, S. Mori and I. Gupta, *Dalton Trans.*, 2015, **44**, 17209-17221.
15. M. Vedamalai, D. Kedaria, R. Vasita, S. Mori and I. Gupta, *Dalton Trans.*, 2016, **45**, 2700-2708.
16. H. Xiang, J. Cheng, X. Ma, X. Zhou and J. J. Chruma, *Chem. Soc. Rev.*, 2013, **42**, 6128-6185.
17. A. Al-Sheikh-Ali, K. S. Cameron, T. S. Cameron, K. N. Robertson and A. Thompson, *Org. Lett.*, 2005, **7**, 4773-4775.
18. S. Kusaka, R. Sakamoto and H. Nishihara, *Inorg. Chem.*, 2014, **53**, 3275-3277.

19. M. Tsuchiya, R. Sakamoto, S. Kusaka, Y. Kitagawa, M. Okumura and H. Nishihara, *Chem. Commun.*, 2014, **50**, 5881-5883.
20. M. Tsuchiya, R. Sakamoto, M. Shimada, Y. Yamanoi, Y. Hattori, K. Sugimoto, E. Nishibori and H. Nishihara, *Inorg. Chem.*, 2016, **55**, 5732-5734.
21. C. Adachi, M. A. Baldo, S. R. Forrest, S. Lamansky, M. E. Thompson and R. C. Kwong, *Appl. Phys. Lett.*, 2001, **78**, 1622-1624.
22. W.-K. Chu, C.-C. Ko, K.-C. Chan, S.-M. Yiu, F.-L. Wong, C.-S. Lee and V. A. L. Roy, *Chem. Mater.*, 2014, **26**, 2544-2550.
23. A. J. Amoroso, M. P. Coogan, J. E. Dunne, V. Fernandez-Moreira, J. B. Hess, A. J. Hayes, D. Lloyd, C. Millet, S. J. Pope and C. Williams, *Chem. Commun.*, 2007, **29**, 3066-3068.
24. K. K.-W. Lo, K. H.-K. Tsang and K.-S. Sze, *Inorg. Chem.*, 2006, **45**, 1714-1722.
25. J. L. Lin, C. W. Chen, S. S. Sun and A. J. Lees, *Chem. Commun.*, 2011, **47**, 6030-6032.
26. K. K.-W. Lo, K. Y. Zhang and S. P.-Y. Li, *Eur. J. Inorg. Chem.*, 2011, **2011**, 3551-3568.
27. F. He, Y. Zhou, S. Liu, L. Tian, H. Xu, H. Zhang, B. Yang, Q. Dong, W. Tian, Y. Ma and J. Shen, *Chem. Commun.*, 2008, **33**, 3912-3914.
28. X. Yi, J. Zhao, J. Sun, S. Guo and H. Zhang, *Dalton Trans.*, 2013, **42**, 2062-2074.
29. T. M. McLean, J. L. Moody, M. R. Waterland and S. G. Telfer, *Inorg. Chem.*, 2012, **51**, 446-455.
30. D. Perl, S. W. Bisset and S. G. Telfer, *Dalton Trans.*, 2016, **45**, 2440-2443.
31. A. Leonidova and G. Gasser, *ACS Chem. Biol.*, 2014, **9**, 2180-2193.
32. J. Bhuvaneswari, P. M. Mareeswaran, S. Shanmugasundaram and S. Rajagopal, *Inorg. Chim. Acta*, 2011, **375**, 205-212.
33. K. Wähler, A. Ludewig, P. Szabo, K. Harms and E. Meggers, *Eur. J. Inorg. Chem.*, 2014, **2014**, 807-811.
34. T. Sainuddin, J. McCain, M. Pinto, H. Yin, J. Gibson, M. Hetu and S. A. McFarland, *Inorg. Chem.*, 2016, **55**, 83-95.
35. L. D. Ramos, H. M. da Cruz and K. P. Morelli Frin, *Photochem. Photobiol. Sci.*, 2017, **16**, 459-466.
36. B. J. Littler, M. A. Miller, C.-H. Hung, R. W. Wagner, D. F. O'Shea, P. D. Boyle and J. S. Lindsey, *J. Org. Chem.*, 1999, **64**, 1391-1396.
37. L. Yu, K. Muthukumaran, I. V. Sazanovich, C. Kirmaier, E. Hindin, J. R. Diers, P. D. Boyle, D. F. Bocian, D. Holten and J. S. Lindsey, *Inorg. Chem.*, 2003, **42**, 6629-6647.
38. M. R. Waterland, T. J. Simpson, K. C. Gordon and A. K. Burrell, *J. Chem. Soc., Dalton Trans.*, 1998, 185-192.
39. J. L. Smithback, J. B. Helms, E. Schutte, S. M. Woessner and B. P. Sullivan, *Inorg. Chem.*, 2006, **45**, 2163-2174.
40. S. G. Telfer, T. M. McLean and M. R. Waterland, *Dalton Trans*, 2011, **40**, 3097-3108.
41. T. M. McLean, D. M. Cleland, S. J. Lind, K. C. Gordon, S. G. Telfer and M. R. Waterland, *Chem. Asian J.*, 2010, **5**, 2036-2046.
42. J. Jayabharathi, V. Thanikachalam and R. Sathishkumar, *New J. Chem.*, 2015, **39**, 235-245.
43. K. Hanson, A. Tamayo, V. V. Diev, M. T. Whited, P. I. Djurovich and M. E. Thompson, *Inorg. Chem.*, 2010, **49**, 6077-6084.
44. V. S. Thoi, J. R. Stork, D. Magde and S. M. Cohen, *Inorg. Chem.*, 2006, **45**, 10688-10697.
45. S. C. Marker, S. N. MacMillan, W. R. Zipfel, Z. Li, P. C. Ford and J. J. Wilson, *Inorg. Chem.*, 2018, **57**, 1311-1331.
46. A. A. Abdel-Shafi, J. L. Bourdelande and S. S. Ali, *Dalton Trans.*, 2007, **24**, 2510-2516.
47. G. Zhang, H. Zhang, Y. Gao, R. Tao, L. Xin, J. Yi, F. Li, W. Liu and J. Qiao, *Organometallics*, 2013, **33**, 61-68.
48. M. Yadav, A. K. Singh, B. Maiti and D. S. Pandey, *Inorg. Chem.*, 2009, **48**, 7593-7603.
49. M. Pineiro, A. L. Carvalho, M. M. Pereira, A. M. d. A. R. Gonsalves, L. G. Arnaut and S. J. Formosinho, *Chem. Eur. J.*, 1998, **4**, 2299-2307.
50. D. Maeda, H. Shimakoshi, M. Abe and Y. Hisaeda, *Inorg. Chem.*, 2009, **48**, 9853-9860.
51. S.-y. Takizawa, R. Aboshi and S. Murata, *Photochem. Photobiol. Sci.*, 2011, **10**, 895-903.
52. T. Fei, X. Gu, M. Zhang, C. Wang, M. Hanif, H. Zhang and Y. Ma, *Synth. Met.*, 2009, **159**, 113-118.
53. A. B. Tamayo, B. D. Alleyne, P. I. Djurovich, S. Lamansky, I. Tsyba, N. N. Ho, R. Bau and M. E. Thompson, *J. Am. Chem. Soc.*, 2003, **125**, 7377-7387.
54. H. D. Tabba, J. A. S. Cavaleiro, D. Jeyakumar, M. Graca, P. M. S. Neves and K. M. Smith, *J. Org. Chem.*, 1989, **54**, 1943-1948.
55. J. M. Sutton, E. Rogerson, C. J. Wilson, A. E. Sparke, S. J. Archibald and R. W. Boyle, *Chem. Commun.*, 2004, **11**, 1328-1329.
56. N. Balsukuri, M. Y. Lone, P. C. Jha, S. Mori and I. Gupta, *Chem. Asian J.*, 2016, **11**, 1572-1587.
57. S. Grimme, J. Antony, S. Ehrlich and H. Krieg, *J. Chem. Phys.*, 2010, **132**, 154104.
58. A. D. Becke, *J. Chem. Phys.*, 1993, **98**, 5648-5652.
59. C. Lee, W. Yang and R. G. Parr, *Phys. Rev. B*, 1988, **37**, 785-789.
60. A. Bergner, M. Dolg, W. Küchle, H. Stoll and H. Preuß, *Mol. Phys.*, 1993, **80**, 1431-1441.
61. Gaussian 09, Revision D.01, M. Frisch, G. Trucks, H. Schlegel, G. Scuseria, M. Robb, J. Cheeseman, G. Scalmani, V. Barone, B. Mennucci, G. Petersson, H. Nakatsuji, M. Caricato, X. Li, H. Hratchian, A.Izmaylov, J. Bloino, G. Zheng, J. Sonnenberg, M. Hada, M. Ehara, K. Toyota, R. Fukuda, J. Hasegawa, M. Ishida, T. Nakajima, Y. Honda, O. Kitao, H. Nakai, T. Vreven, J. A. Montgomery, Jr., J. Peralta, F. Ogliaro, M. Bearpark, J. Heyd, E. Brothers, K. Kudin, V. Staroverov, T. Keith, R. Kobayashi, J. Normand, K. Raghavachari, A. Rendell, J. Burant, S. Iyengar, J. Tomasi, M. Cossi, N. Rega, J. Millam, M. Klene, J. Knox, J. Cross, V. Bakken, C. Adamo, J. Jaramillo, R. Gomperts, R. Stratmann, O. Yazyev, A. Austin, R. Cammi, C. Pomelli, J. Ochterski, R. Martin, K. Morokuma, V. Zakrzewski, G. Voth, P. Salvador, J. Dannenberg, S. Dapprich, A. Daniels, O. Farkas, J. Foresman, J. Ortiz, J. Cioslowski, and D. Fox, Inc., Wallingford, CT, 2009.
62. M. Cossi, N. Rega, G. Scalmani and V. Barone, *J. Comput. Chem.*, 2003, **24**, 669-681.
63. M. E. Casida, in *Recent Advances In Density Functional Methods: (Part I)*, World Scientific, 1995, pp. 155-192.
64. R. Dennington, T. Keith and J. Millam, *Semichem Inc.: Shawnee Mission, KS*, 2009.

Journal Name ARTICLE

TOC

View Article Online
DOI: 10.1039/C8DT04540B